Automated Lane Changing with a Controlled Steering-Wheel Feedback Torque for Low Lateral Acceleration Purposes

Automated Lane Changing With a Controlled Steering-Wheel Feedback Torque for Low Lateral Acceleration Purposes

Jan Loof, Igo Besselink, and Henk Nijmeijer, *Fellow, IEEE*

***Abstract*—To bridge the gap between autonomous and normal steering during low lateral acceleration maneuvers, a steering-wheel torque controller is developed. It consists of three controllers in series, a high-gain feedback steering-wheel torque controller, a nonlinear steering-angle controller, and a linear yaw-rate controller. A validated two degrees of freedom steering-system model, in combination with a single-track vehicle model, is used to determine the controller parameters. Driving tests with different drivers have been executed to find a comfortable steering-wheel torque/angle relation. This relation is maintained throughout the lane change by specifying the steering-wheel torque as a function of the steering-wheel angle tracking error. Experiments show promising results regarding the driver/vehicle interaction, but also show that a system to detect the lanes and the vehicle position on the road is required for further improvement.**

***Index Terms*—Electric power-steering, steering-wheel feedback torque, yaw-rate control, steering-system model, lane change, autonomous driving.**

I. Introduction

THE steering-wheel feedback torque is an important clue for the driver to determine the current vehicle state [1], [2]. While it is important for the driver to receive information transmitted from the tyre road contact to the steering-wheel, the steering-wheel torque should be confined within a certain range for the driver to be able to comfortably steer the vehicle. This can be achieved with a large reduction ratio from the steering-wheel to the front wheels, but this would result in excessive steering-wheel angles. To resolve this, many passenger vehicles are equipped with a power-steering system which aids the driver by amplifying the steering-wheel torque torque applied by the driver. In general, power-steering systems use a torque sensor to sense the driver applied steering-wheel torque and use either a hydraulic or an electric actuator to provide the torque amplification. Fig. 1 shows an example of an electric power-steering (EPS) system where the electric motor is placed on the steering-rack. The electronic control unit (ECU) uses the torque sensor output and controls the electric motor assistance torque.

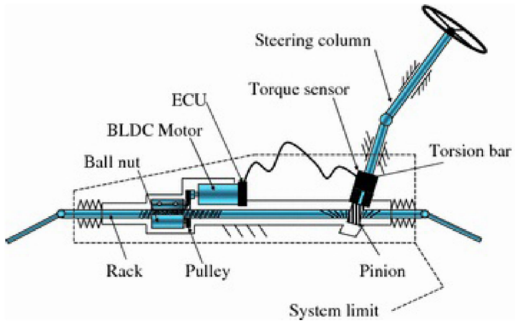

Fig. 1. Electric power-steering system with a rack assist example [3].

Modern cars utilize the power-steering system for more than just reducing the torque levels. In [4], the electric power-steering-system of a passenger is utilized for obstacle avoidance, where yaw-rate tracking is used to control the vehicle motion. A reference path is generated and a resulting yaw-rate reference is tracked. Experiments show that this system can be used to avoid obstacles even with high lateral accelerations. In [5], [6] the electric power-steering system of a passenger vehicle is used to control the steering angle in the context of platooning by using a camera to track the license plate of a preceding vehicle. A lateral controller is developed based on the a look-ahead vector as a virtual control point. A driver intervention system can detect when the driver resists the motion and the system should be switched off, via the steering-wheel torque sensor. Reference [7] analyzes the stability of a passenger vehicle equipped with a lane-keeping system with uncertainty in the driver behavior. Where [4] and [5], [6] mainly focus on fully automated driving, [7] sees lane keeping more as a shared steering control where the vehicle and the driver are working together. In [8] and [9] this concept of shared control is researched more in depth by means of a driving simulator. It is concluded that it is important that the human agrees with the actions of the automation and it should be avoid that the human starts ”fighting” the automation system. This also shows that one cannot successfully develop a system which has to interact with a human, without doing experiments with humans in the loop.

The control of EPS systems is a broadly studied subject, in conventional EPS systems the steering-wheel torque is sensed

Manuscript received February 21, 2018; revised June 12, 2018 and December 11, 2018; accepted March 21, 2019. Date of publication August 28, 2019; date of current version November 21, 2019. This research was supported by the Netherlands Organisation for Scientific Research (NWO) under Grant 12831. *(Corresponding author: Jan Loof.)*

The authors are with the Department of Mechanical Engineering, Eindhoven University of Technology, 5612 AZ Eindhoven, The Netherlands (e-mail: j.loof@tue.nl; i.j.m.besselink@tue.nl; h.nijmeijer@tue.nl).

Color versions of one or more of the figures in this article are available online at http://ieeexplore.ieee.org.

Digital Object Identifier 10.1109/TIV.2019.2938097

by a flexible element and amplified. To make the steering-wheel return to the neutral position a self centering function is often super imposed on top of the power-steering assist [3]. In [10] it is shown that the torque sensor can be eliminated from the system and an estimator can be used to estimate the steering-wheel torque. It is also shown in this paper that amplifying this estimated torque to reduce the steering-wheel torque does reduce the steering-wheel torque but can also lead to vibrations. Even though this paper presents successful results, it is not applied in vehicles on the market at this time. An idea for a controller which merges the steering-wheel torque control and steering-wheel angle control into one is presented in [11] but only in a simulation and without experiments.

As a part of the Dutch project "Truck Merging Support", a lane changing assistant for trucks is developed [12]. In most autonomous steering vehicles, there is a clear distinction between the autonomous steering mode, where the vehicle is in control, and the manual steering-mode, where the driver is in control. Also in most autonomous steering vehicles the vehicle is completely in control and it is not well defined what the driver experiences in terms of steering-wheel feedback torque upon regaining control. In this project, a steering-system torque controller is designed for the purpose of changing lanes with a truck where the driver can always take over control. As a testing platform for the steering-system controller for the commercial vehicle, a passenger vehicle is utilized and the controller is adapted to the passenger vehicle. Because trucks tip over at low lateral accelerations, the scope of this paper is limited to low lateral accelerations. Because the project scope is merging on the motor-way, a constant forward velocity comparable to speeds on the motor-way is considered. This leads to the following research question:

Develop a control strategy for an electric power-steering system in a passenger vehicle which is able to control the lateral vehicle motion during low lateral accelerations and constant highway velocity, while at the same time allowing the driver to intervene.

The main contribution of this paper compared to existing literature is:

Development of a lane-changing support system with steering-wheel feedback torque control.

The main difference with existing literature is a non-linear relation between the steering-wheel feed-back torque and deviation from the desired steering angle. No on or off switching of the controller is required and the steering-wheel torque is always well defined and manageable for the driver in contrast to [4]–[6]. In this way a shared control between the driver and the vehicle is achieved and experiments with a real vehicle are shown instead of a driving simulator [11].

The outline of this paper is as follows. In Section II, a control strategy is proposed where the steering-wheel torque is directly controlled as a function of the steering-wheel angle. The torque controller is connected in series with a yaw-rate controller. In Section III a steering-system model is developed and parametrized. This model is utilized to find the controller parameters. Driving tests are performed to find a nominal steering-wheel feedback torque profile. Additional driving tests with the complete control strategy in place are presented in this section as well. Section IV discusses the results obtained. The conclusions and recommendations are given in Section V. An overview of the nomenclature can be found in Table I.

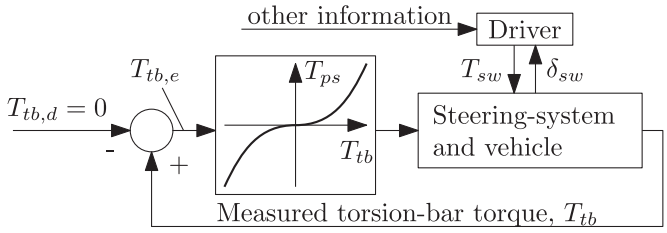

Fig. 2. Control scheme of a conventional power-steering system.

II. Control Strategy

A conventional EPS system can be considered as a positive feedback control scheme as shown in Fig. 2. The steering-wheel torque is measured by using a flexible element, often referred to as the torsion-bar. The deflection of this bar in combination with the known stiffness results in the torsion-bar torque measurement T_{tb}. In the feedback scheme a non-linear dependency of the power-steering assist torque T_{ps} on T_{tb} is used. Often a progressive characteristic is applied, where the power-steering gradient increases with an increasing torsion-bar torque. Because the desired torsion-bar torque $T_{tb,d}$ is zero in this control scheme, the torsion-bar torque T_{tb} equals the error $T_{tb,e} = T_{tb} - T_{tb,d}$. The driver interacts with the steering-system by applying a steering-wheel torque T_{sw} based on δ_{sw} and other information such as the position on the road for example.

In the proposed controller, the desired torsion-bar torque $T_{tb,d}$ is not zero and is tracked by a high-gain feed-back controller. The following subsections describe first the steering-wheel feedback torque controller, the angle controller and the combination with a yaw-rate controller.

A. Steering-Wheel Feedback Torque Controller

Fig. 3 shows the control scheme for the steering-wheel feedback torque. The power-steering torque T_{ps} is determined by a high-gain linear feedback controller controller $C_{tb}(s)$. In the Laplace domain with the Laplace variable s, we obtain:

$$T_{ps}(s) = (T_{tb} - T_{tb,d}(s))C_{tb}(s) = T_{tb,e}(s)C_{tb}(s). \quad (1)$$

The goal of this torque controller is to track a desired torsion-bar torque $T_{tb,d}$, i.e. $\lim_{t\to\infty} T_{tb,e} = 0$. Note the difference between Figs. 3 and 2 where $T_{tb,d} = 0$, the feedback controller is a non-linear gain and not necessarily aiming for perfect tracking.

Most EPS systems measure the steering-column angle δ_{sc}, that is said, the angle downstream of the torque sensor, in other words on the wheel side. A a trade-off has to be made between good tracking of a desired steering-column angle $\delta_{sc,d}$ and leaving the option open for the driver to intervene. A non-linear dependency of the desired torsion-bar torque $T'_{tb,d}$ on the steering-column angle error $\delta_{sc,e} = \delta_{sc,d} - \delta_{sc}$ is used. To have a smooth continuous function, an arc-tangent function, with an additional slope for large errors is used:

$$T'_{tb,d} = b\text{atan}(a\delta_{sc,e}) + c\delta_{sc,e}. \quad (2)$$

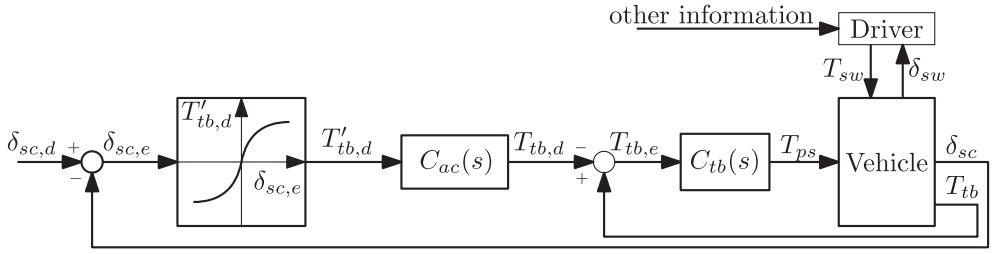

Fig. 3. Steering-wheel feedback torque controller.

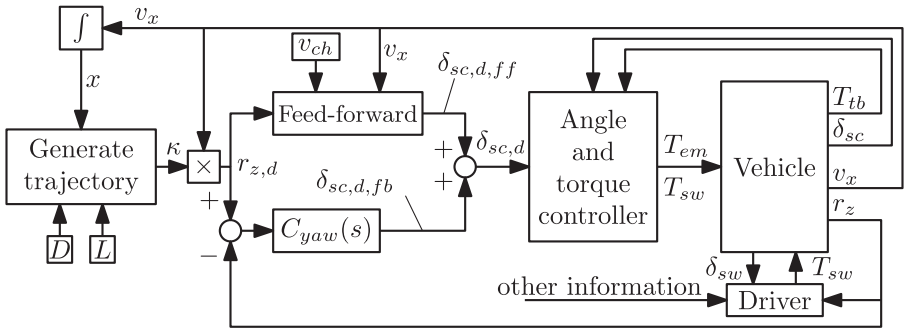

Fig. 4. Yaw-rate control scheme including trajectory generator. The block "angle and torque controller" contains the control scheme from Fig. 3. The goal is to track the generated trajectory.

This function has a slope of $ab + c$ for small values of $\delta_{sc,e}$ and c for large values, i.e.:

$$\left.\frac{\partial T'_{tb,d}}{\partial \delta_{sc,e}}\right|_{\delta_{sc,e}=0} = ab + c, \quad \left.\frac{\partial T'_{tb,d}}{\partial \delta_{sc,e}}\right|_{\delta_{sc,e}=\infty} = c. \tag{3}$$

To ensure sufficient damping of the system, the filter $C_{ac}(s)$ is used: $T_{tb,d}(s) = T'_{tb,d}(s)C_{ac}(s)$.

B. Yaw-Rate Controller

The yaw-rate of the vehicle is controlled according to the control scheme of Fig. 4. The angle and torque controller block contains the control scheme of Fig. 3. The yaw-rate controller is based on the work of [4], but with a different angle and torque controller. A lateral displacement path y_d is generated according to the lane width D and the length of the lane change L as a function of the traveled distance x [13]:

$$y_d(x) = D\left(10\left(\frac{x}{L}\right)^3 - 15\left(\frac{x}{L}\right)^4 + 6\left(\frac{x}{L}\right)^5\right). \tag{4}$$

The curvature κ of this path can be calculated by using the following expression [13]:

$$\kappa(x) = \frac{\frac{\partial^2 y_d(x)}{\partial x^2}}{\left(1 + \left(\frac{\partial y_d(x)}{\partial x}\right)^2\right)^{3/2}}. \tag{5}$$

The desired vehicle yaw-rate $r_{z,d}$ to follow this path is obtained by multiplying the curvature with the forward velocity v_x:

$$r_{z,d}(x) = \kappa(x)v_x. \tag{6}$$

An example of a generated path and the corresponding desired yaw-rate is shown in Fig. 5. To track this desired yaw-rate,

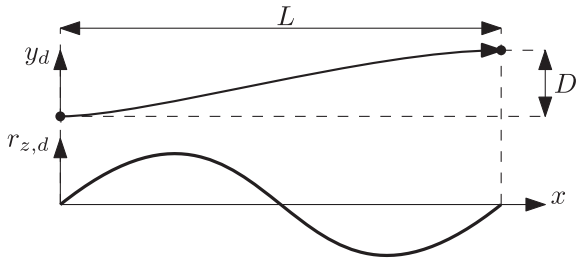

Fig. 5. Example of a generated path with desired lateral displacement y_d and the corresponding desired yaw-rate $r_{z,d}$ as a function of traveled distance x.

the desired steering-column angle $\delta_{sc,d}$ has to be calculated. The characteristic velocity v_{ch} is defined as the speed for an understeered vehicle where the steer angle needed to negotiate a turn is twice the Ackermann angle. By using knowledge about the current vehicle velocity, a feed-forward steering-column reference angle $\delta_{sc,d,ff}$ can be calculated based on the steady-state yaw-velocity gain of the single track vehicle model [14] as:

$$\delta_{sc,d,ff} = \frac{l}{v_x}\left(1 + \left(\frac{v_x}{v_{ch}}\right)^2\right) r_{z,d} i_w \tag{7}$$

where i_w is the ratio between the steering-angle of the front-wheels and the steering-wheel. To compensate for imperfections in the road, such as banking, rutted roads, sidewind etc., a linear feedback controller $C_{yaw}(s)$ is used to calculate $\delta_{sc,d,fb}$ based on the tracking error $r_{z,e} = r_{z,d} - r_z$ and written in the Laplace domain as:

$$\delta_{sc,d,fb}(s) = C_{yaw}(s)r_{z,e}(s). \tag{8}$$

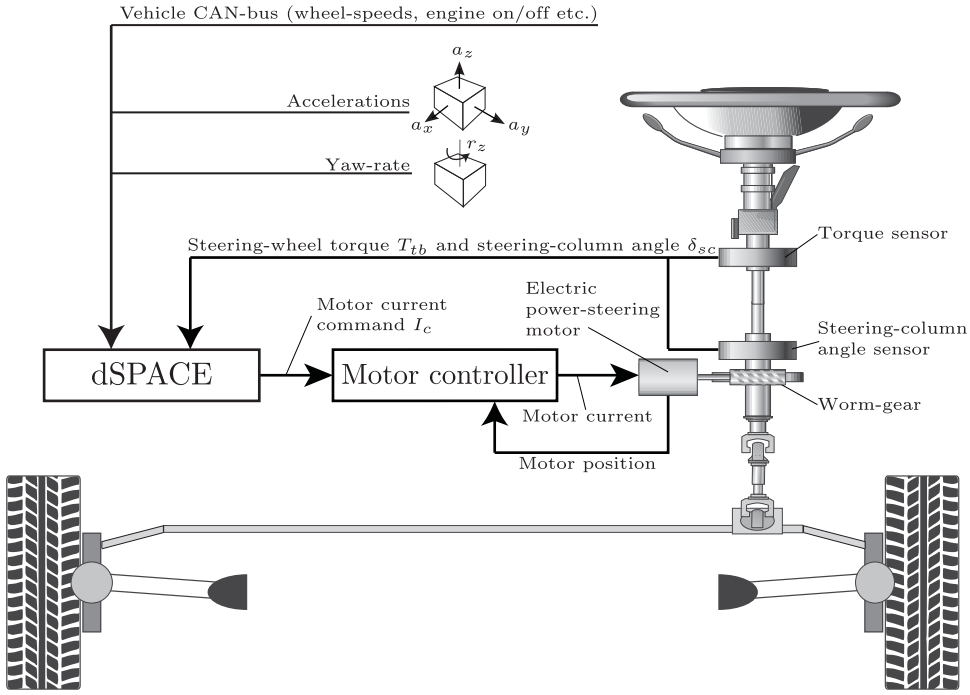

Fig. 6. Overview of the steering-system and additional sensors of the test vehicle.

The desired steering-angle $\delta_{sc,d}$ is the sum of the feed-forward and feed-back:

$$\delta_{sc,d} = \delta_{sc,d,ff} + \delta_{sc,d,fb}. \tag{9}$$

III. Implementation

In this research, a passenger vehicle with an EPS system is used (VW Lupo 3L, [5]). Fig. 6 shows the steering-system layout with the additional hardware and sensor signals. The assistance motor is installed on the steering-column with a reduction ratio $i_{em} = 22$, downstream of the torque sensor. A dSPACE platform processes the measured signals, such as the steering-column angle δ_{sc} and the steering-wheel torque T_{tb}. An inertial measurement unit (IMU) measures the acceleration in three directions and the yaw-rate r_z. The wheel-speeds are obtained from the vehicle CAN-bus. The vehicle speed v_x is calculated by the average of the four wheel-speeds. The phase cables and encoder cables of the electric motor are connected to a custom motor controller, Elmo Drum Gold 70/48, to directly control the motor current I_q and thus the electric motor torque T_{em} via a current command I_c. The motor current control loop has a bandwidth of 2.5 kHz and is therefore T_{em} is assumed to be instantaneously available when a current command I_c is given.

A. Steering-System Model

To design the controllers $C_{tb}(s)$ and $C_{ac}(s)$, a steering-system model is utilized. Passenger car EPS systems are often modeled using two degrees of freedom (DOF), [11] where everything upstream of the torsion-bar is lumped into one equivalent inertia J_{sw} with angle δ_{sw} which represents the first degree of freedom. Because the electric motor has a large reduction ratio i_{em}, the steering-rack mass and wheel inertia are neglected and only the

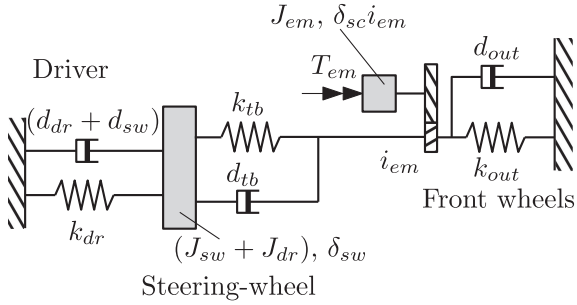

Fig. 7. The two degrees of freedom steering-system model including driver model.

electric motor inertia J_{em} is relevant [3] and considered the second degree of freedom. The dominant stiffness in the system is the torque sensor, which has stiffness k_{tb}. The approach from [15] is used to include the driver. A spring-damper system with k_{dr} and d_{dr} respectively and added inertia because of the drivers' arms J_{dr}. When the driver is absent, $d_{dr} = k_{dr} = J_{dr} = 0$. The damping constants d_{sw} and d_{out} represent absolute damping of the steering-wheel and the steering-column and the damping constant d_{tb} represents relative damping between the steering-wheel and steering-column. A stiffness k_{out} is used to model the self centering effect of the steering-system due to the king-pin inclination and caster angle of the vehicle. The model is shown in Fig. 7 and is described by the following equations of motion:

$$\begin{aligned}(J_{sw} + J_{dr})\ddot{\delta}_{sw} = &-k_{tb}(\delta_{sw} - \delta_{sc}) - d_{tb}(\dot{\delta}_{sw} - \dot{\delta}_{sc}) \\ &- k_{dr}\delta_{sw} - \dot{\delta}_{sw}(d_{dr} + d_{sw}) \end{aligned} \tag{10}$$

$$\begin{aligned}J_{em} i_{em}^2 \ddot{\delta}_{sc} = &-k_{tb}(\delta_{sc} - \delta_{sw}) - d_{tb}(\dot{\delta}_{sc} - \dot{\delta}_{sw}) \\ &- k_{out}\delta_{sc} - \dot{\delta}_{sc} d_{out} + T_{em} i_{em} \end{aligned} \tag{11}$$

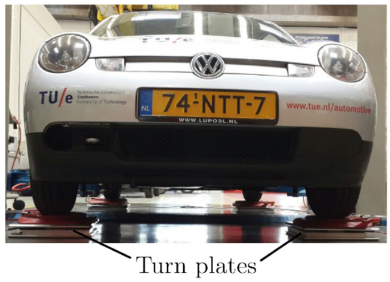

Fig. 8. Test vehicle in the laboratory with the wheels on quasi frictionless turn-plates.

and can be written in a linear state-space system as:

$$\dot{\underline{x}} = \underline{A}\ \ \underline{x} + \underline{B}\ \ \underline{u}, \qquad \underline{y} = \underline{C}\ \ \underline{x} \tag{12}$$

with the state vector $\underline{x} = \begin{bmatrix} \dot{\delta}_{sw} & \delta_{sw} & \dot{\delta}_{sc} & \delta_{sc} \end{bmatrix}^T$, the input $\underline{u} = T_{em}$ and the outputs $\underline{y} = \begin{bmatrix} \delta_{sc} & T_{tb} \end{bmatrix}^T$. The system matrix $\underline{A}$ is defined as:

$$\underline{A} = \begin{bmatrix} 0 & 1 & 0 & 0 \\ -\frac{k_{tb}+k_{dr}}{J_{sw}} & -\frac{d_{tb}+d_{dr}+d_{sw}}{J_{sw}} & \frac{k_{tb}}{J_{sw}} & \frac{d_{tb}}{J_{sw}} \\ 0 & 0 & 0 & 1 \\ \frac{k_{tb}}{J_{em}i_{em}^2} & \frac{d_{tb}}{J_{em}i_{em}^2} & \frac{k_{tb}+k_{out}}{J_{em}i_{em}^2} & \frac{d_{tb}+d_{out}}{J_{em}i_{em}^2} \end{bmatrix} \tag{13}$$

and the input matrix $\underline{B}$ and output matrix $\underline{C}$ are defined as:

$$\underline{B} = \begin{bmatrix} 0 \\ 0 \\ 0 \\ \frac{1}{J_{em}} \end{bmatrix}, \qquad \underline{C} = \begin{bmatrix} 0 & 0 & 1 & 0 \\ -k_{tb} & 0 & k_{tb} & 0 \end{bmatrix} \tag{14}$$

The transfer function from the input $\underline{u}$ to the output $\underline{y}$ is calculated as $\underline{C}(s\underline{I} - \underline{A})^{-1}\underline{B}$ where $\underline{I}$ is the unity matrix of proper dimensions.

B. Model Identification

To identify the parameters of the steering-system model, frequency response measurements (FRFs) are used. To incorporate both the scenarios of a driver holding the steering-wheel and the driver not holding the steering-wheel and to investigate the effect of a driving vehicle or a vehicle in the laboratory with the wheels supported on frictionless turn-plates, as shown in Fig. 8, three measurements are executed:

1) No driver present, vehicle in the laboratory.
2) Driver present and holding the steering-wheel thoroughly, vehicle in the laboratory .
3) Driver present and providing the necessary guidance to drive straight at a speed of 50 km/h.

During these measurement the input amplitude is limited to $T_{em} = 0.5$ Nm and a sinusoidal chirp signal with a frequency content from 1 to 50 Hz is used for a duration of 240 seconds. The sampling time is 0.001 seconds. Fig. 9 shows the transfer function estimates. The difference between the measurement with and without driver is significant, with the driver in the loop, the system is more damped and the first resonance frequency moves to a lower frequency, from 12 to 7 Hz. The difference

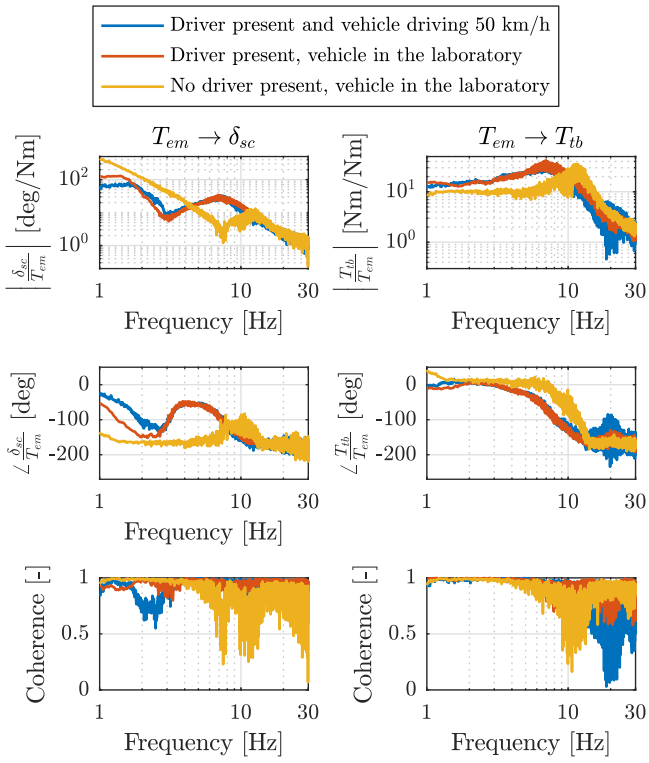

Fig. 9. Measured transfer functions from T_{em} to δ_{sc} and T_{tb} under different circumstances.

between the vehicle being in the laboratory or driving on the road is small, only in the region close to 1 Hz differences can be seen, but this can also be caused by the driver behaving differently. The measurement where the vehicle is driving is not further used in this paper, since the laboratory measurement is of better quality. From here onwards the driver being absent is referred to as scenario 1 and the driver holding the steering-wheel is referred to as scenario 2. Some of the model parameters can be measured directly (i_{em}, k_{tb} and k_{out}), others can be estimated by rules of thumb or literature (J_{dr} ,J_{em}, J_{sw}, k_{dr} and d_{dr}) and the remaining parameters are tuned by hand to obtain a good correlation between the model and the measurement. Fig. 10 shows the transfer functions from electric motor torque to both steering-column angle and torsion-bar torque. The measured responses from Fig. 9 are shown together with the steering system with the parameters from Table II. A good correspondence with the measurements is seen.

C. Controller Parameters

With the verified steering-system model, the parameters for the controller $C_{tb}(s)$ and $C_{ac}(s)$ can be determined. The transfer function from T_{em} to T_{tb} is referred to as $G_u(s)$ and $G_c(s)$ depending on the driver presence where u stands for unconstrained, so no driver and c stands for constrained, so with the driver holding the steering-wheel. Based on the bode-plots shown in Fig. 11 and the design requirement of $\lim_{t\to\infty} T_{tb,e} = 0$ a controller with a proportional gain $K_{p,tb}$ is used in combination with a lead filter with filter frequencies ω_{l1} and ω_{l2}:

$$C_{tb}(s) = K_{p,tb}\frac{\omega_{l1}^{-1}s + 1}{\omega_{l2}^{-1}s + 1}. \tag{15}$$

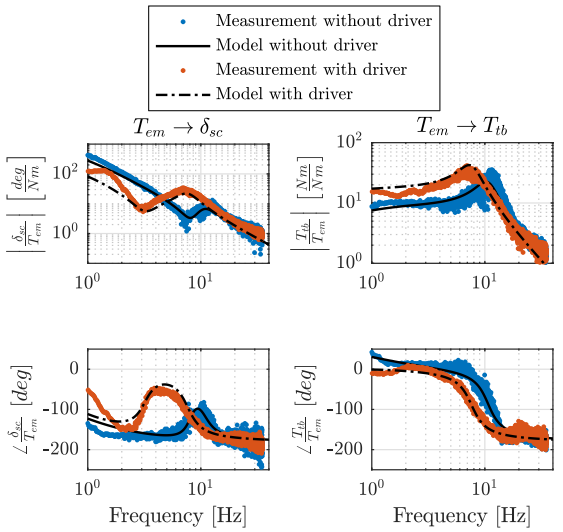

Fig. 10. Steering-system model transfer functions in comparison with the measurements.

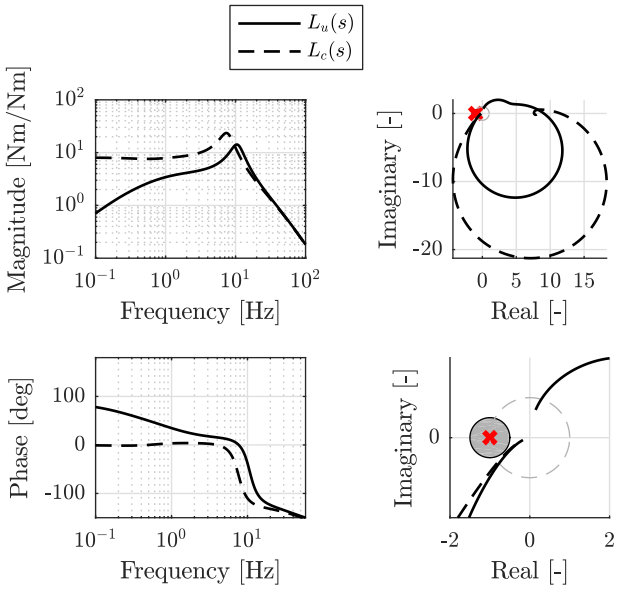

Fig. 11. Bode-plots of the open-loop transfer functions $L_u(s)$ and $L_c(s)$ on the left side. The right side graphs show the Nyquist plots of these same transfer functions.

The lead filter frequencies are chosen at $\omega_{l1} = 26\pi$ rad/s and $\omega_{l2} = 80\pi$ rad/s to increase the phase in a large frequency region. The proportional gain $K_{p,tb} = 10 i_{em}^{-1}$ is chosen as high as possible, while not exceeding the actuator limits. Fig. 11 shows the open-loop transfer functions $L_i(s) = C_{tb}(s)G_i(s)$ with $i \in \{u, c\}$, which show a bandwidth of 40 Hz stability according to the Nyquist criterion and robust stability margins, phase margin $>$ 30 degrees, modulus margin $<$ 2 and gain margin $>$ 2 [16]. Stability of the system can also be checked using the Nyquist plot in the right side of figure.

The desired steering torque characteristic is determined by means of experiments with drivers on the road. The experiments have been executed with 10 drivers in the age range of 25–30 years old. All drivers have a drivers license for at least 5 years and have a technical background as a PhD candidate or post-doctoral researcher in the field of mechanical engineering. The

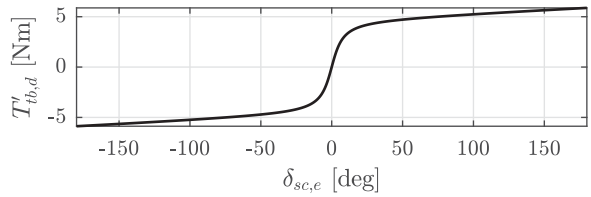

Fig. 12. Experimentally determined steering-wheel torque characteristic.

experiments have been executed on a sunny days in the months July and August, where the outside temperatures were between 20 and 30 degrees Celsius. The drivers each executed 10 lane-changes over a time span of approximately 5 minutes, where they could choose when they wanted to change lanes. At the same time the function parameters a, b and c are changed based on questions asked. The drivers are questioned regarding the straight-line stability and the steering-effort. If the straight-line stability is lacking, a is increased to increase the slope around the origin while maintaining similar maximum torque levels. When the steering-effort is too high, b is decreased to lower the inflection point in the vertical direction which reduces the steering-effort. After the experiments, the parameters $a = 9.74$, $b = 3$ Nm/rad and $c = 0.4$ Nm/rad are obtained, resulting in the torque profile of Fig. 12. Around the origin, this function has a slope of 0.517 Nm/deg and for large values of $\delta_{sc,e}$ the slope is 0.007 Nm/deg.

Because the curve from Fig. 12 only acts on the angle error and not on the derivative(s), the necessity for dampening of the system is reviewed. The transfer functions from $T_{tb,d}$ to δ_{sc} with the torque controller active are used to design the dynamic filter on the angle controller. The filter uses an under-damped second order low-pass filter to make the phase change at 8 Hz less abrupt and to increase the phase in the region between 1 and 8 Hz, a PD controller is used:

$$C_{ac}(s) = \frac{\omega_d^{-1} s + 1}{\omega_{lp}^{-2} s^2 + 2\beta_{lp}\omega_{lp}^{-1} s + 1} \tag{16}$$

with $\omega_d = 3\pi$ rad/s, $\omega_{lp} = 16\pi$ rad/s and $\beta_{lp} = 0.25$. Fig. 13 shows $C_{ac}(s)$ multiplied with the gain of $(ab + c)$ which occurs at $\delta_{sc,e} = 0$ and multiplied with the gain of c which occurs for large $\delta_{sc,e}$. The open-loop transfer functions $L_{ac,i}(s) = (ab + c)C_{ac}(s)G_{tc,i}(s)$ show a bandwidth of 5 Hz when the driver is absent ($i = u$) and 1.5 Hz when the driver is present ($i = c$) when $\delta_{sc,e}$ is small. For large values of $\delta_{sc,e}$, the bandwidth is negligible, but the system is still stable. All cases show stability according to the Nyquist criterion and robust margins. Since this paper focuses on the steering-torque profile mainly, the reader is referred to [12] for a more detailed analysis on the design of the dynamic filter. Most passenger vehicles have a peak in the transfer function from steering-angle to yaw-rate around 1 Hz, after this peak the phase starts decreasing. The transfer function from steering-column angle to yaw-rate is referred to as $G_{yaw}(s)$ and modeled by a single-track model. For parameters and a description of this model a reference is made to [12]. The assumption is that the vehicle response has no influence on the steering-system dynamics in this frequency range, the closed loop angle controlled system response $T_{ac,i}(s) = \frac{L_{ac,i}(s)}{1+L_{ac,i}(s)}$ can be multiplied with $G_{yaw}(s)$ to obtain the transfer function from

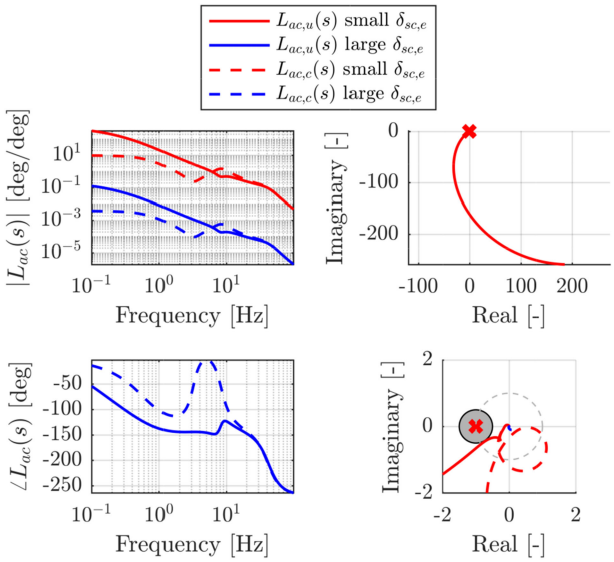

Fig. 13. Bode-plots of the open-loop transfer functions $L_{ac,u}(s)$ and $L_{ac,c}(s)$. The right side of the figure shows the Nyquist plots.

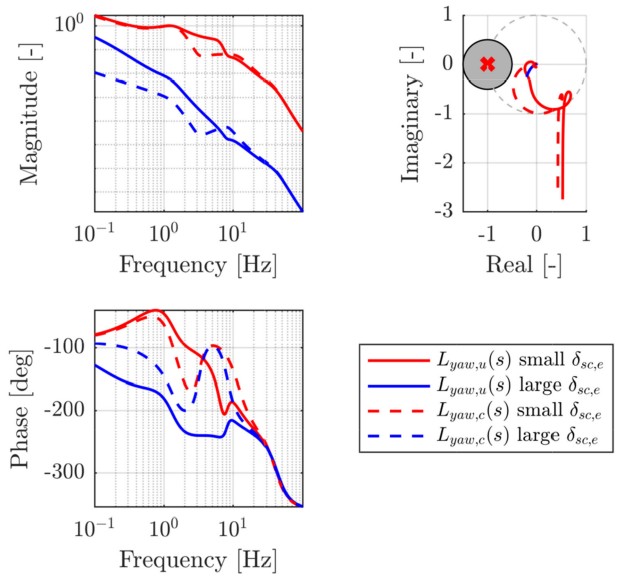

Fig. 14. Bode-plots of the open-loop transfer functions $L_{yaw,u}(s)$ and $L_{yaw,c}(s)$. The right side of the figure shows the Nyquist plots.

steering-angle command $\delta_{sc,d}$ to yaw-rate:

$$G_{yaw,i}(s) = G_{yaw}(s)T_{ac,i}(s) \qquad \text{with} \qquad i \in \{u, c\} \tag{17}$$

The yaw-rate controller is designed for a velocity of 165 km/h, this is the top-speed of a VW Lupo and is considered worst case because the yaw-rate response becomes less dampened with increasing forward velocity. The yaw-rate responses including the steering-system dynamics and controllers $G_{yaw,i}$ show a significant amount of phase lag after 1 Hz, compared to G_{yaw}. Based on this phase lag a PI controller is used with the breaking point not exceeding 1 Hz and making sure to choose the P-action such that the bandwidth for the situation without the driver is close to 1 Hz:

$$C_{yaw}(s) = K_{p,yaw}\left(1 + \frac{K_{i,yaw}}{s}\right) i_w \tag{18}$$

with $K_{p,yaw} = 0.1$, $K_{i,yaw} = 2\pi$. The open-loop transfer functions $L_{yaw,i}(s)$ obtained by $C_{yaw}(s)G_{yaw,i}(s)$ are plotted in Fig. 14. A bandwidth of 1 Hz is obtained with robustness margins for small values of $\delta_{sc,e}$. For large values of $\delta_{sc,e}$, stability is maintained according to the Nyquist criterion with robust margins. Also for more details on the yaw-rate feed-back controller, the reader is referred to [12].

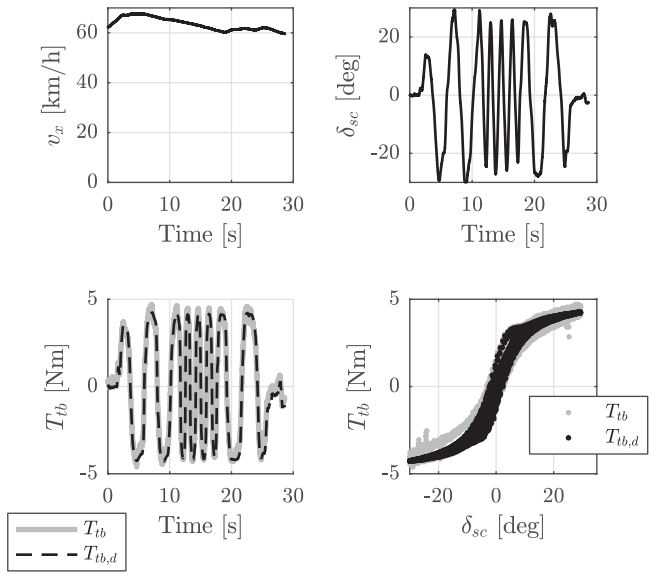

Fig. 15. An experiment without the yaw-rate controller where $\delta_{sc,d} = 0$ and the driver provides a sinusoidal steering-input with a variable frequency content.

D. Experiments

Two experiments are presented in this paper. In the first experiment the yaw-rate controller is not used and the focus is on the control scheme of Fig. 3. The reference angle $\delta_{sc,d} = 0$ during this experiment. The driver provides a sinusoidal steering-wheel input with a variable frequency content as shown in the top-right graph of Fig. 15. The bottom-left graph shows the desired and actual torsion-bar torque as a function of time. It confirms that the desired torsion-bar torque is tracked accurately. The bottom-right graph shows the desired and actual torsion-bar torque as a function of the steering-column angle. Because $\delta_{sc,d} = 0$, this graph looks similar to Fig. 12. Some hysteresis is present in the desired torsion-bar torque because of the dynamic $C_{ac}(s)$, which provides some damping to the system.

In the second experiment a lane change is performed with $L = 100$ meters and $D = 4$ meters. A second person (not the driver) initiates the lane-change and in this experiment the driver is accepting the lane-change by following the steering-wheel torque guidance. The vehicle is not equipped with a lateral displacement sensor, but an estimate of the lateral displacement y_{est} is made based on the forward velocity v_x, yaw-rate r_z and the lateral acceleration a_y. By rewriting the equations of motion of the single track vehicle model the lateral position

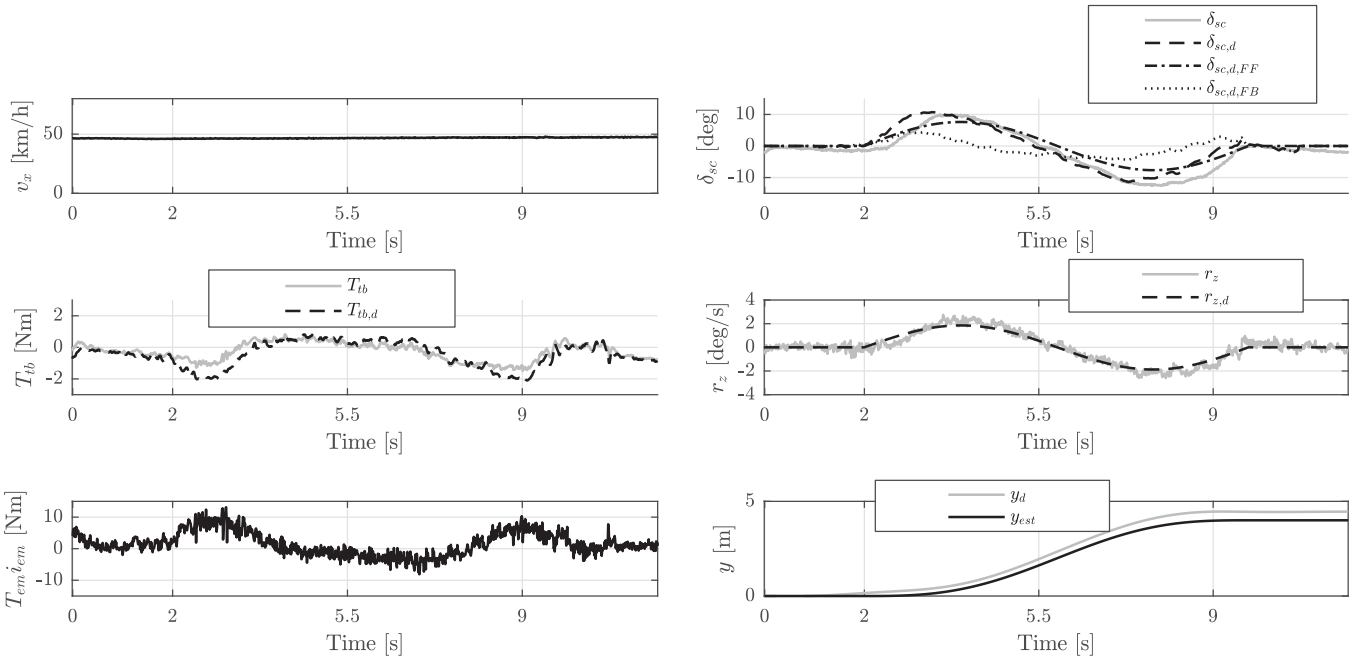

Fig. 16. A lane-change experiment where the driver is accepting the guidance.

y_{est} can be obtained:

$$a_y = \dot{v}_y + v_x r_z \quad \rightarrow \quad \dot{v}_{y,est} = a_y - v_x r_z \tag{19}$$

$$v_{y,est} = \int \dot{v}_{y,est} dt \tag{20}$$

$$y_{est} = \int v_{y,est} dt. \tag{21}$$

Fig. 16 shows the results of this test. The vehicle is maintaining a speed of 50 km/h throughout the maneuver. The bottom-right graph shows a smooth profile where the desired lateral displacement y_d goes from 0 to 4 meters in 7 seconds, starting at $t = 2$ s and ending at $t = 9$ s. The middle right graph shows the measured yaw-rate and the reference yaw-rate which shows that the vehicle in combination with the driver is able to track the yaw-rate accurately. The top-right graph shows the steering-column angle δ_{sc}, the desired steering-column angle $\delta_{sc,d}$ and the feedback and feed-forward component, $\delta_{sc,d,fb}$ and $\delta_{sc,d,ff}$ respectively. This graph shows that initially the driver is providing a non-zero steering-angle while driving straight already. Throughout the maneuver the contribution of the feedback and feed-forward is almost equal. The torsion-bar torque is plotted in the middle-left graph and remains small during this maneuver ($|T_{tb}| < 2$ Nm), indicating that the driver is complying with the maneuver. The bottom-left graph shows the electric motor torque T_{em} multiplied with the reduction ratio to the column i_{em}, a peak assistance torque of 12 Nm is generated under these circumstances. The lateral position estimation y_{est} shows that the vehicle follows the desired trajectory. Some deviation at the end is seen, but it is unclear if this is caused by drift of the sensor or an actual error since the sensor signals are integrated twice to obtain the lateral position y_{est}. This example shows that the driver is able to cooperate with the steering-controller. Additional tests have been performed but because of lack of space the reader is referred to [12] where an experiment is shown where the driver does not comply. In that experiment the steering-wheel torque does not exceed an absolute value of 4 Nm which is deemed manageable for a driver.

IV. Discussion

The goal of this paper is to control the vehicle motion by means of a specified steering-wheel torque feed-back controller and a yaw-rate controller while still allowing the driver to intervene. A series connection of three controllers is utilized: a torque controller, an angle controller and a yaw-rate controller. The controllers are developed using a validated a steering-system model and a single-track vehicle model. As a torque controller a high-gain proportional feed-back controller is used with a lead-lag filter resulting in a bandwidth of 40 Hz. Based on the dynamics of the system, one would expect that PID controller could perform better and this control structure is also used in [11]. This approach results however in hunting [17] because of the coulomb friction level of 2 Nm in the test vehicle. Others use the feed-back of other sensor signals such as the motor velocity [18], [19]. This is not necessary if one can actuate and measure at a high sampling frequency (1 kHz in our vehicle). As an angle controller, [11] proposed a gain with a saturation. This results in a un-natural feeling for the driver because of the sudden change in gradient and a continuously differentiable function is advised. The experiment without the yaw-rate controller shows a good tracking of the torque controller and the torque-angle relation feels comfortable as reported by multiple drivers. The two degree of freedom steering-system model where the steering-wheel is separated from the wheels and connected by the torsion-bar is a good representation of the reality. Additional degrees of freedom are not necessary in the measured frequency range (30 Hz). The yaw-rate controller is currently not dependent of the vehicle velocity, in case of a lower forward velocity the yaw-rate controller gains can be increased. During the experiments this does not seem necessary but can be used in case of tracking problems. During the experiments there was no feedback from

the actual lateral position on the road, resulting in the system not being very robust to faulty initial conditions or not perfectly straight roads. Position feedback of a camera or any other lateral position detection system could improve this, since camera systems often have low update frequency and significant delay, a feedback loop using only the camera position might not function well. By using the lateral position to correct the desired yaw-rate, a fast control loop for the yaw-rate can still utilized and small corrections to the desired path can be applied by using the camera feedback.

V. Conclusion and Recommendation

The steering-system of a VW Lupo 3L, equipped with electro-mechanical power-steering, can be modeled with a linear two degrees of freedom model within the range of 1 to 30 Hz. One degree of freedom represents the steering-wheel and the other represents the wheel angle and the electric motor. A significant amount of dry friction is present, but given a large enough input amplitude, the steering-system can be approximated as being linear. A driver can be modeled as an additional spring-damper system attached to the steering-wheel, with additional inertia added to the steering-wheel, representing the arms of the driver. Within the range of 2 to 30 Hz this is an accurate representation. Below 2 Hz, non-linear effects such as friction become more important. To guide the driver during automated steering, a steering angle controller, which has a non-linear dependency between the steering-wheel torque and steering angle, proves to be useful. By using a combination of a high stiffness close to the desired steering angle and a low stiffness further away from the desired angle, the driver can be guided, but still feels in control of the steering-wheel. Combining the steering angle controller with a yaw-rate controller can be used to guide the vehicle during a lane-change. During normal driving the reference angle is set to straight-line driving. In this way no controllers are switched on or off when transitioning from straight-line driving to a lane-change and vice versa. Experiments with the VW Lupo 3L are used to derive comfortable steering-wheel torque setpoints. At this moment the setpoints are the authors choice. A more systematic approach, with for example a questionnaire, could provide better setpoints. A controller for merging and changing lanes is developed and tested. A similar controller architecture might prove useful for a lane-keeping assist. Especially because no switching of controllers is necessary to initiate a lane-change.

During this research, the longitudinal vehicle control is not considered. Including longitudinal control in the algorithm could make the controller suitable for other autonomous maneuvers as well such as: overtaking, weaving, diverging and evasive maneuvers. In this research only low lateral accelerations are considered because the controller is designed for a merging assistant for a truck. If this control strategy is applied for higher lateral accelerations, the steering-wheel torque profile has to be adjusted by increasing the slope around zero steering-angle and increasing the maximum torque, allowing less room for the driver to intervene. In this paper, no feed-back of the lateral position on the road is used. A sensor to measure the real position on the road, for example a camera, could be used to improve the lane-changing algorithm. Only straight roads are considered in this paper, this could be resolved by changing the yaw-rate set-point as shown in [13]. This has not been tested since the scope of this paper lies on the interaction with the driver and showing a proof of concept of the presented control strategy. This paper assumes that the planned trajectory is tracked and the trajectory is not updated when this is not the case. A deviation from the path would result in the controller trying to push the driver back to the desired path. Because of the non-linear relation between the steering-wheel torque and angle this would result in a manageable torque levels. No driver detection algorithm is used in the experiments with the VW Lupo 3L. With this controller architecture, a driver intervention detection based on the steering-angle tracking error could work without the need of extra sensors.

Appendix
Nomenclature and Steering-System Model Parameters

TABLE I
Nomenclature

Filter damping	β
Angle	δ
Curvature	κ
Frequency	ω
Lateral acceleration	a_y
Torque profile constants	a, b and c
Width of a lane	D
Controller gain	K
Length to perform a lane change	L
Yaw-rate	r_z
Torque	T
Velocity	v
Longitudinal position	x
Lateral position	y
Angle controlled	Subscript ac
Driver present and not present	Subscripts c and u
Characteristic	Subscript ch
Desired	Subscript d
Error	Subscript e
Electric motor	Subscript em
Estimated	Subscript est
Feedforward and feedback	Subscripts FF and FB
Low-pass filter	Subscript lp
Proportional and integral	Subscripts p and i
Steering-wheel	Subscript sw
Steering-column	Subscript sc
Torsion-bar	Subscript tb
Torque controlled	Subscript tc
Longitudinal, lateral and vertical direction	Subscripts x, y, z
Controller transfer function	$C(s)$
Plant transfer function	$G(s)$
Open-loop transfer function	$L(s)$
Closed-loop transfer function	$T(s)$

TABLE II
Parameters of the Steering-System Model

Damping provide by the driver	d_{dr}	$26.2 \cdot 10^{-3}$ Nms/deg
Damping on the wheel side	d_{out}	$8.7 \cdot 10^{-3}$ Nms/deg
Damping of the torque sensor	d_{tb}	$7.9 \cdot 10^{-3}$ Nms/deg
Damping on the steering-wheel	d_{sw}	$1.7 \cdot 10^{-3}$ Nms/deg
Assistance motor reduction ration	i_{em}	22
Driver inertia	J_{dr}	0.20 kgm^2
Assistance motor inertia	J_{em}	$1 \cdot 10^{-4}$ kgm^2
Steering-wheel inertia	J_{sw}	0.03 kgm^2
Torque sensor stiffness	k_{tb}	1.6 Nm/deg
Driver stiffness	k_{dr}	3.7 Nm/deg
Jack torque gradient	k_{out}	0.015 Nm/deg

ACKNOWLEDGMENT

The research was executed at Eindhoven University of Technology.

REFERENCES

[1] D. Toffin, G. Reymond, A. Kemeny, and J. Droulez, "Role of steering wheel feedback on driver performance: Driving simulator and modeling analysis," *Vehicle Syst. Dyn.*, vol. 45, no. 4, pp. 375–388, 2007.
[2] D. Toffin, G. Reymond, A. Kemeny, and J. Droulez, "Influence of steering wheel torque feedback in a dynamic driving simulator," in *Proc. Driving Simul. Conf.*, North America, Dearborn, MI, USA, 2003.
[3] M. Harrer and P. Pfeffer, *Steering Handbook*. Wiesbaden, Germany: Springer, 2016.
[4] J. Shah, M. Best, A. Benmimoun, and M. Ayat, "Autonomous rear-end collision avoidance using an electric power steering system," *Proc. Institution Mech. Engineers Part D: J. Automobile Eng.*, vol. 229, no. 12, pp. 1638–1655, 2015.
[5] E. Kruijswijk, "Towards automated steering for vehicle platooning," in *Proc. Int. Symp. Adv. Vehicle Control*. Technische Universiteit Eindhoven, 2012. [Online]. Available: https://research.tue.nl/en/publications/towards-automated-steering-for-vehicle-platooning
[6] E. Kruijswijk, "Towards automated steering for vehicle platooning," Master's thesis, Eindhoven Univ. Technology, Eindhoven, The Netherlands, 2012.
[7] L. Saleh, P. Chevrel, F. Claveau, J. Lafay, and F. Mars, "Shared steering control between a driver and an automation: Stability in the presence of driver behavior uncertainty," *Trans. Intell. Transp. Syst.*, vol. 14, no. 2, pp. 974–983, 2013.
[8] D. Abbink, M. Mulder, and E. Boer, "Haptic shared control: Smoothly shifting control authority?" *Cognition Technol. Work*, vol. 14, no. 1, pp. 19–28, 2012.
[9] D. Katzourakis *et al.*, "Shared control for road departure prevention," in *Proc. Int. Conf. Syst. Man Cybern.*, IEEE, 2011, pp. 1037–1043.
[10] K. Yamamoto, D. Koenig, O. Sename, and P. Moulaire, "A new control design for an optimized electric power steering system," in *Proc. IFAC World Congress*, 2017. [Online]. Available: http://hal.univ-grenoble-alpes.fr/hal-01597586/document.
[11] J. Kim and J. Song, "Control logic for an electric power steering system using assist motor," *Mechatronics*, vol. 12, no. 3, pp. 447–459, 2002.
[12] J. Loof, "Modeling and control of a truck system for active driver support," Ph.D. dissertation, Eindhoven Univ. Technology, Eindhoven, The Netherlands, 2018.
[13] W. Nelson, "Continuous-curvature paths for autonomous vehicles," in *Proc. Int. Conf. Robot. Autom.*, IEEE, 1989, pp. 1260–1264.
[14] H. Pacejka, *Tire and Vehicle Dynamics*. Oxford, U.K.: Elsevier, 2005.
[15] A. Pick and D. Cole, "Neuromuscular dynamics and the vehicle steering task," *Dyn. Vehicles Roads Tracks*, vol. 41, pp. 182–191, 2003.
[16] D. Bruijnen, R. van de Molengraft, and M. Steinbuch, "Optimization aided loop shaping for motion systems," in *Proc. Int. Symp. Intell. Control.*, IEEE, 2006, pp. 255–260.
[17] R. Wu and P. Tung, "Studies of stick-slip friction, presliding displacement, and hunting," *J. Dyn. Syst. Meas. Control*, vol. 124, no. 1, pp. 111–117, 2002.
[18] W. Zhaojian, G. Konghui, Z. Jianwei, D. Haitao, and C. Shuang, "Experimental study on anti-vibration of EPS," in *Proc. Int. Conf. Comput. Mechatronics Control Electron. Eng.*, IEEE, 2010, vol. 3, pp. 292–295.
[19] H. Henrichfreise, J. Jusseit, and H. Niessen, "Optimale regelung einer elektromechanischen servolenkung," *VDI Berichte*, vol. 1753, pp. 381–400, 2003.

Jan Loof received the M.Sc. degree in mechanical engineering from the Eindhoven University of Technology, Eindhoven, The Netherlands, in 2013. He is working toward the Ph.D. degree in the Dynamics and Control group at the Department of Mechanical Engineering, Eindhoven University of Technology, under the supervision of Prof. H. Nijmeijer and Dr. I. Besselink. His research was part of the NWO project *Truck merging support*, focusing on improving safety in trucks by active driver support during merging on the highway. His main topics were modeling and control of truck steering-system and passenger car steering-system.

Igo Besselink received the graduation in mechanical engineering from the Delft University of Technology, Delft, The Netherlands, in 1990, and received the Ph.D. degree from the TU Delft in 2000.

He is an Associate Professor with the Eindhoven University of Technology, Eindhoven, The Netherlands. Thereafter he joined the Fokker Aircraft and became responsible for the analysis of landing gear design loads and stability. In 1996, he joined the TNO automotive, Delft, and was responsible for tyre simulation software development and various projects related to vehicle dynamics. In 2002, he was a part-time Lecturer in the field of vehicle dynamics in the Dynamics and Control group of Prof. Henk Nijmeijer. In 2008, he became full-time employed as an Assistant Professor with the Eindhoven University of Technology. In January 2016, he was appointed as Associate Professor, while still being a member of the Dynamics and Control group. His research interests include tyre modeling, dynamics of commercial vehicles, vehicle control, and battery electric vehicles.

Henk Nijmeijer received the M.Sc. and Ph.D. degrees in mathematics from the University of Groningen, Groningen, The Netherlands. He is a Full Professor with the Eindhoven University of Technology, Eindhoven, The Netherlands, and chairs the Dynamics and Control group. He has published a large number of journal and conference papers, and several books.

Dr. Nijmeijer is/was a member of the editorial board of numerous journals. He is an Editor of *Communications in Nonlinear Science and Numerical Simulations*. He was awarded the IEE Heaviside premium in 1990. He is appointed Honorary Knight of the "golden feedback loop" (NTNU) in 2011. Since 2011, he has been an IFAC Council Member. From January 2015, he has been a Scientific Director of the Dutch Institute of Systems and Control (DISC). He is recipient of the 2015 IEEE Control Systems Technology Award. He is program leader of the Dutch research program "Integrated Cooperative Automated Vehicles" (i-CAVE). Since April 2017, he has been the Director of the Graduate Program Automotive Technology of the Eindhoven University of Technology.